J. Min. Metall. Sect. B-Metall. 49 (3) B (2013) 245 - 256

Journal of Mining and Metallurgy, Section B: Metallurgy

A LUMP-INTEGRAL MODEL BASED FREEZING AND MELTING OF A BATH MATERIAL ONTO A CYLINDRICAL ADDITIVE OF NEGLIGIBLE RESISTANCE

U.C. Singh[a,*], A. Prasad[b,^], A. Kumar[c,Δ]

[a]Engineering Division, Tata Steel Limited, Business centre, Bistupur, Jamshedpur, India
[b]Department of Mechanical Engineering, National Institute of Technology, Jamshedpur, India
[c]Department of Mechanical Engineering, Birla institute of Technology Mesra, Ranchi, India

(Received 08 August 2012; accepted 04 April 2013)

Abstract

In a theoretical analysis, a lump-integral model for freezing and melting of the bath material onto a cylindrical additive having its thermal resistance negligible with respect to that of the bath is developed. It is regulated by independent non-dimensional parameters, namely the Stefan number, S_t the heat capacity ratio, C_r and the modified conduction factor, C_{ofm}. Series solutions associated with short times for time variant growth of the frozen layer and rise in interface temperature between the additive and the frozen layer are obtained. For all times, numerical solutions concerning the frozen layer growth with its melting and increase in the interface temperature are also found. Time for freezing and melting is estimated for different values of C_r, S_t and C_{ofm}. It is predicted that for lower total time of freezing and melting $C_{ofm}<2$ or $C_r<1$ needs to be maintained. When the bath temperature equals the freezing temperature of the bath material, the model is governed by only C_r and S_t and gives closed-form expressions for the growth of the frozen layer and the interface temperature. For the interface attaining the freezing temperature of the bath material the maximum thickness of the frozen layer becomes $\xi_{max} = \sqrt{C_r(C_r + S_t)}$. The model is validated once it is reduced to a problem of heating of the additive without freezing of the bath material onto the additive. Its closed-form solution is exactly the same as that reported in the literature.

Keywords: Additive addition; Melt-additive system; Mathematical modeling; Freezing and melting.

1. Introduction

Production of steel and cast iron of different grades at low cost with increased productivity and without compromise of quality has gained great importance owing to much global competition. For any grade of these, alloying materials and scraps of various sizes and shapes, called solid additives are assimilated in the hot metal known as bath to prepare the melt of requisite composition. Other process phases are then followed. Here, the assimilation of the additive in the bath undergoes a complex phenomenon that constitutes several phases. In the first phase, soon after the additive is immersed in the bath, freezing of the bath material onto the surface of the additive initiates with the interface between the additive and the frozen layer attaining an instant equilibrium temperature and the heat begins to penetrate the additive. With the passage of time, the frozen layer grows in thickness and both the temperature at the interface and the heat penetration depth increase. Subsequently, the frozen layer melts but the interface temperature and the heat penetration depth continue to increase. Ultimately, the frozen layer completely melts exposing the additive at an elevated temperature. The second phase comprises of heating of the additive to its melting temperature. In the third phase, it melts and assimilates in the bath. The three phases are accomplished in a certain time and are functions of geometry and temperature of the additive, temperature and condition of the bath and thermo-physical properties of the additive-bath system. This time controls the productivity of the product. For increasing the productivity, its reduction is essential. It can be achieved once the time taken in the undesirable first phase of freezing and melting of the bath material onto the additive in the assimilation process is decreased. The occurrence of the first phase is caused by the development of a steep temperature gradient towards the additive side of the interface soon after its immersion in the bath resulting in heat conducted to the additive far greater than the convective heat supplied by the bath. The

* *Corresponding author: umeshchandra.singh@tatasteel.com; ^ Retired Professor; [Δ] Professor and Head*

DOI:10.2298/JMMB120808028S

remaining amount of the conductive heat is balanced by the latent heat of fusion liberated owing to the freezing of the bath material around the additive. With passing of the time this heat raises the interface temperature and decreases the temperature gradient and the rate of the growth of the frozen layer. Eventually, the heat conducted diminishes to such an amount that the convective heat from the bath melts completely the frozen layer uncovering the additive at an elevated temperature. Since the temperature gradient in the first phase is dependent upon the order of magnitude of the thermal resistance of the additive compared with that of the frozen layer and the bath, the later becomes the regulating factor for the time taken in the first phase and, in turn, the total time of these phases.

A low value of the ratio of these two resistances known as the Biot number, B_i decreases the temperature gradient towards the additive side and requirement of the conductive heat. These permit completion of freezing and melting of the bath material in a lesser time. Further reduction in this time is possible if the additive of negligible thermal resistance represented by $B_i<0.1$ that establishes a uniform temperature in it is taken. The literature seldom reports such a situation that is frequently encountered in practice. However, freezing and melting of the bath material onto the plate [1], cylindrical [2] and spherical [3] shaped additives was investigated for the comparable thermal resistance of the additives with respect to those of the frozen layer onto these additives. They are implicitly related to $0.1<Bi<100$. In this condition, it was shown that the time of freezing and melting of the bath material around the cylindrical [4-8] additive made of steel [4], titanium [5-7], niobium [8] and zirconium [9] decreased once the radius of the cylindrical additive reduced. The akin result was also obtained for decreasing radius of the cored cylindrical wire injected in the steel bath [10]. Decreased radius of the spherical additive of aluminum in a salt-melt bath [11], slag in slag melt [3] and ferro-magnese in steel bath [12] diminished the time of freezing of the bath material with its subsequent melting. This time was also obtained theoretically for the freezing and melting of the iron melt bath material around the spherical shaped sponge iron [13] and ferromanganese [14] when the temperature of the frozen layer of bath material was assumed to be uniform. In the latter situation [14], the ferromanganese spherical particles were fed continuously into the bath with the size distribution employed from [15]. The mathematical model for melting and mixing of alloys addition was also devised [16]. For the development of the interface temperature at the interface between the cylindrical additive and the growing frozen layer of the bath material onto the additive immediately after dunking it in the bath, the present authors [17] provided a closed-form expression. Such an expression was also found for the same phenomenon in case of plate shaped additive [18]. Closed-form solutions for the frozen layer thickness, its maximum thickness, their time of growth and the time of the freezing and melting were recently obtained by the present authors [19] when the freezing and melting of the bath material occurred onto the cylindrical additive in an agitated bath. Here, a thin frozen layer having negligible thermal resistance and uniform temperature was developed. For this situation, laboratory experiment data for the growth of the frozen layer of the steel melt bath onto the porous ferromolybdenum cylinders of different densities during their melting and dissolution [20] were obtained and compared with the model results [21].

The present study concerns the development of a lump-integral model related to freezing with its subsequent melting of a bath material onto a cylindrical additive in a bath-additive system. The thermal resistance of the additive is taken as negligible with respect to that of the bath including the frozen layer. The model indicates the dependence of this phenomenon on the independent nondimensional parameters, the Stefan number, S_t, the modified conduction factor, C_{ofm}, and the heat capacity ratio, C_r. The effect of these parameters upon this phenomenon is examined graphically. For the bath to be at the freezing temperature of the bath material, the model gives closed-form solutions for the interface temperature and the frozen layer. From this, the closed-form expression for the maximum frozen layer is deduced when the interface temperature attains the freezing temperature of the bath material. The model is validated once it is converted to a problem of transient heating of a cylindrical body having its thermal resistance negligible with respect to that of the surroundings.

2. Formulation of the problem

A cylindrical shaped solid additive at an initial temperature, T_{ai} is considered. Its significant radius is r_{as} defined by the ratio of its volume and the surface area. Such an additive is immersed in a melt bath maintained at a uniform temperature, T_b greater than the melting or freezing temperature, T_{mf} of the bath material. Immediately the bath material freezes around the surface of the additive and the contact interface between the frozen layer and the additive attains an equilibrium temperature, T_e that lies between the initial temperature of the additive and its melting temperature, T_{af} larger than the freezing temperature, T_{mf} of the bath material. Moreover, the bath-cylindrical solid additive system sets up a

temperature field, Fig.1, $T_{ai}<T_e<T_{mf}<T_{af}<T_b$. As the time of immersion elapses, the temperature, T_e rises, the heat penetrates radially to the cylindrical additive and the axisymmetric growth of the frozen layer takes place when the rate of heat conduction from the frozen layer to the additive remains more than the convective heat available to the frozen layer from the bath. Once these two rates become equal, the growth of the frozen layer ceases. Beyond this time, owing to the convective heat from the bath to the frozen layer greater than conductive heat from the frozen layer to the additive, the frozen layer begins to melt but the interface equilibrium temperature, T_e continues to increase with further heating of the additive. At time $t=t_{mc}$, the frozen layer completely melts leaving the additive at an elevated temperature, T_{em} ($T_{em}<T_{mf}$).

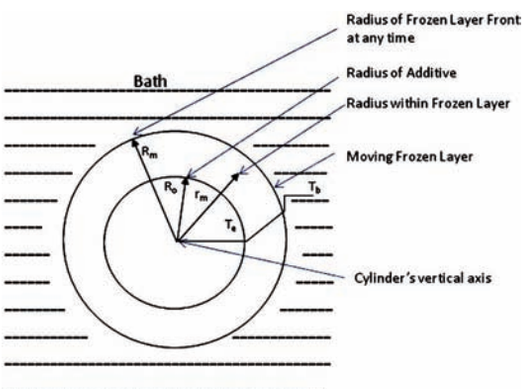

Figure 1. *Schematic of freezing of bath material onto the cylindrical shaped solid additive of negligible resistance in bath.*

This phenomenon is simulated by axisymmetric conjugated unsteady heat conduction. The nondimensional integral form of heat conduction equation applied to the frozen layer takes the following form.

$$\frac{d}{d\tau}\int_{C_r}^{\xi}\xi_m\theta_m d\xi_m-\left(\xi_m\theta_m\right)_{\xi_m=\xi}\frac{d\xi}{d\tau}+\left(\xi_m\theta_m\right)_{\xi_m=C_r}\frac{dC_r}{d\tau}=$$
$$=\left(\xi_m\frac{\partial\theta_m}{\partial\xi_m}\right)_{\xi_m=\xi}-\left(\xi_m\frac{\partial\theta_m}{\partial\xi_m}\right)_{\xi_m=C_r},\quad C_r<\xi_m<\xi\ ,\tau>0 \quad (1)$$

Physically, the first term of the right hand side of Eq.(1) represents the rate of heat conducted in the frozen layer through the freezing boundary surface at $\xi_m=\xi$ and the second term, the rate of heat conducted out of the frozen layer to the additive through the contact interface at $\xi_m=C_r$. The difference of these two, the net rate of conducted heat is responsible for increasing the net rate of internal thermal energy of the frozen layer provided by left hand side of Eq.(1). Its first term implies the rate of increase in the thermal energy of the frozen layer whereas the combination of its second and third terms is indicative of the rate of acquired internal thermal energy due to the rate of increase in the volume of the frozen layer.

Related initial and boundary conditions for Eq.(1) are

$$\theta_m=\theta_b,\ \xi_m=C_r,\ \tau=0 \quad (2)$$

$$\theta_m=\theta_e,\ \xi_m=C_r,\ \tau>0 \quad (3)$$

$$\frac{\partial\theta_m}{\partial\xi_m}=\frac{1}{BC_{of}}+\frac{1}{S_t}\frac{\partial\xi}{\partial\tau},\qquad \theta_m=1,\ \xi_m=\xi,\ \tau>0 \quad (4)$$

If the cylindrical solid additive is assumed to be of small radius r_o and large length, l, its thermal resistance becomes negligible with respect to convective thermal resistance of the bath and the conductive thermal resistance of the growing frozen layer. This characteristic establishes a uniform temperature in the entire volume of the additive which is equal to the contact interface temperature, T_e between the additive and the frozen layer. The additive behaves as a lump system [22, 23]. To this system the application of an energy balance between the heat conducted to the lump from the frozen layer through the contact interface and the increase in the thermal energy of the lump provides.

$$\frac{\partial\theta_e}{\partial\tau}=-\frac{2q_{na}}{B} \quad (5)$$

Its initial condition is

$$\theta_a=\theta_e=0,\ 0<\xi_a<1,\ \tau=0 \quad (6)$$

The interface conjugating conditions between the additive and the frozen layer lead to

$$K_{ma}\xi_m\frac{\partial\theta_m}{\partial\xi_m}=-\xi_a q_{na},\qquad \xi_m=C_r,\ \xi_a=1,\ \tau>0 \quad (7)$$

$$\theta_m=\theta_a=\theta_e,\ \xi_m=C_r,\qquad \xi_a=1,\ \tau>0 \quad (8)$$

Here, Eqs.(1) to (8) constituting the mathematical model of lump-integral form are written when the thermo-physical properties of the additive and the frozen layer are uniform but different. This form is arrived on the basis of the additive acting as a lump and the frozen layer behaving as an integral system in the direction of its growth. Equations (7) and (8) assume the surface of the cylindrical additive in perfect contact with the surface of the frozen layer. Also no interface resistance exists between them. Such assumptions taken in the recent studies for freezing of the bath material onto the spherical [3] and plate [1] shaped additives of comparative thermal resistance of the additive with respect to the frozen layer yielded reliable results.

Note that equations (1) to (8) exhibit the dependence of the problem upon independent non-dimensional parameters- C_{of}, the conduction factor, S_t, the Stefan number, B, the property-ratio, C_r, the heat capacity-ratio and K_{ma}, the conductivity-ratio.

3. Solutions

The lump-integral model just developed for the present problem is nonlinear owing to the moving boundary of the frozen layer, Eq.(7) and coupled due to conjugate conditions, Eqs.(7) and (8). These preclude its closed-form solutions employing available exact analyses. In such a case alternative semi analytical methods become important. One of these, the integral method that yielded closed- form expressions pertaining to freezing [24] or melting [25-27] in the previous investigations and reduced [28] similar other problems to initial value problems is applied. In view of this advantage, the equation governing the frozen layer has already been written in the integral form, Eq.(1) which after substitution of Eqs.(3) and (4) reduces it to

$$\frac{d}{d\tau}\int_{C_r}^{\xi}\xi_m\theta_m d\xi_m-\xi\frac{d\xi}{d\tau}= =\left(\xi_m\frac{\partial\theta_m}{\partial\xi_m}\right)_{\xi_m=\xi}-\left(\xi_m\frac{\partial\theta_m}{\partial\xi_m}\right)_{\xi_m=C_r},\ C_r<\xi_m<\xi,\ \tau>0 \quad (9)$$

To find its solutions, a temperature field within the frozen layer needs to be specified. A linear temperature profile that fulfils Eqs.(3) and (4) is chosen.

$$\theta_m=1+(\theta_e-1)\left(1-\frac{\xi_m-C_r}{\xi-C_r}\right) \quad (10)$$

This type of profile is justified since it provided reliable results for phase-change problems [27, 29] in the past. Employing Eq.(10), the integral Eq.(9) takes the form.

$$\frac{d}{d\tau}\left[\frac{1}{2}\left(\xi^2-C_r^2\right)+(\theta_e-1)\left\{-\frac{C_r}{2}(C_r-\xi)+\frac{1}{6}(C_r-\xi)^2\right\}\right]-\xi\frac{d\xi}{d\tau}=\left(\xi_m\frac{\partial\theta_m}{\partial\xi_m}\right)_{\xi_m=\xi}-\left(\xi_m\frac{\partial\theta_m}{\partial\xi_m}\right)_{\xi_m=C_r} \quad (11)$$

It is transformed to

$$\frac{d}{d\tau}\left[\frac{1}{2}\left(\xi^2-C_r^2\right)+(\theta_e-1)\left\{-\frac{C_r}{2}(C_r-\xi)+\frac{1}{6}(C_r-\xi)^2\right\}\right]-\frac{\xi^2}{2}=\frac{\xi}{BC_{of}}+\frac{1}{S_t}\xi\frac{d\xi}{d\tau}+\frac{C_r(\theta_e-1)}{\xi-C_r} \quad (12)$$

when the boundary condition Eq.(4) is applied. Substituting Eq.(10) in the governing Eq.(5) for the additive gives.

$$\frac{d\theta_e}{d\tau}=\frac{2}{B}.K_{ma}\frac{\xi_m}{\xi_a}\frac{\partial\theta_m}{\partial\xi_m}\Big/at\,\xi_m=C_r\,and\,\xi_a=1 \quad (13)$$

whereas use of Eq.(10) reduces it to

$$\frac{d\theta_e}{d\tau}=-\frac{2(\theta_e-1)}{\xi-C_r} \quad (14)$$

Examination of Eq.(12) for the frozen layer ξ indicates that it is coupled with Eq.(14) owing to presence of Θ_e in it. For solutions, these two equations are rearranged in standard format of simultaneous differential equations of first order in time, τ. First Eq.(12) is converted in terms of $\frac{d\xi}{d\tau}$ and $\frac{d\theta_e}{d\tau}$

$$\left[(\theta_e-1)A_1-\frac{\xi}{S_t}\right]\frac{d\xi}{d\tau}+A_2\frac{d\theta_e}{d\tau}=\frac{\xi}{BC_{of}}+\frac{C_r(\theta_e-1)}{\xi-C_r} \quad (15)$$

Where,

$$A_1=\frac{C_r}{2}+\frac{1}{3}(\xi-C_r),\ A_2=\frac{C_r}{2}(\xi-C_r)+\frac{1}{6}(\xi-C_r)^2$$

then Eq.(14) is employed giving

$$\frac{d\xi}{d\tau}=\frac{\xi(\xi-C_r)+BC_{of}(\theta_e-1)(C_r+2A_2)}{(\xi-C_r)\left[(\theta_e-1)A_1-\frac{\xi}{S_t}\right]BC_{of}} \quad (16)$$

Equations (14) and (16) constitute an initial value problem with initial conditions $\xi=C_r$, $\theta_e=0$ at $\tau=0$. As they do not provide closed form solutions even after application of exact analyses and their numerical solutions do not get initiated using the standard fourth order Runge-Kutta method due to the presence of ∞ at the initial conditions, series solutions for small times are resorted to. From these, starting values of ξ and θ_e in the vicinity of $\tau\to0$ (i.e $\tau=10^{-4}$) are found. Computer software of Runge-Kutta method is now enable to calculate numerical values for ξ and θ_e for all times once these starting values are used.

3.1 Series solutions for small times

To find series solutions for small times residing within the vicinity of initial time, τ=0, following series solutions.

$$\xi=\sum_{i=0}^{n}a_i\tau^{i/2} \quad (17)$$

$$\theta_e=\sum_{i=0}^{n}b_i\tau^{i/2} \quad (18)$$

are assumed. They satisfy the initial conditions $\xi=C_r$, $\theta_e=0$ at $\tau=0$ and provide $a_o=C_r$ and $b_o=0$. To quickly determine the coefficients of Eqs.(17) and (18), Eqs.(14) and (16) need to be cast, respectively, in

$$(\xi-C_r)\frac{d\theta_e}{d\tau}+2(\theta_e-1)=0 \quad (19)$$

and

$$BC_{of}(\xi-C_r)\left[(\theta_e-1)A_1-\frac{\xi}{S_t}\right]\frac{d\xi}{d\tau}= =\xi(\xi-C_r)+BC_{of}(\theta_e-1)(C_r+2A_2) \quad (20)$$

before Eqs.(17) and (18) are employed. On application of Matlab, the other coefficients for higher order of τ become

$$a_1 = \pm 2\sqrt{\frac{S_t}{2+S_t}},\ b_1 = \pm 2\sqrt{\frac{2+S_t}{S_t}}$$

$$a_2 = \left[\frac{4}{3}\left(C_{of}C_r - C_r - \frac{2}{3}C_{of}\right)S_t^2 - \frac{8}{3}\left(C_r - C_{of}\right)S_t - \frac{16}{3}C_{of}C_r\right] \Big/ C_{of}C_r\left(2+S_t\right)^2$$

$$b_2 = \left[\frac{2}{3}\left(C_r + \frac{2}{3}C_{of} - 4C_{of}C_r\right)S_t^2 + \left(\frac{4}{3}C_{of} - 8C_{of}C_r + \frac{4}{3}C_r\right)S_t - \frac{16}{3}C_{of}C_r\right] C_{of}C_r S_t\left(2+S_t\right)$$

$$a_3 = \left[\frac{1}{9}\begin{pmatrix} -\frac{10}{3}C_{of}C_r + 2C_r^2 - \frac{26}{3}C_{of}^2C_r - \\ -22C_r^2C_{of} + \frac{80}{9}C_{of}^2 + 2C_{of}^2C_r^2 \end{pmatrix}S_t^4 + \frac{1}{9}\begin{pmatrix} -36C_{of}^2C_r^2 - 98C_r^2C_{of} + \frac{4}{3}C_{of}C_r + \\ +\frac{160}{3}C_{of}^2 + 8C_r^2 - 44C_{of}^2C_r \end{pmatrix}S_t^3 + \frac{1}{9}\begin{pmatrix} -80C_{of}^2 - 128C_r^2C_{of} - 160C_{of}^2C_r + \\ +16C_{of}C_r - \frac{4}{3}C_{of}^2C_r + 8C_r^2 \end{pmatrix}S_t^2 + \right.$$

$$\left. + \frac{1}{9}\left(104C_{of}^2C_r - 144C_{of}^2C_r^2 - 40C_r^2C_{of}\right)S_t + \frac{1}{9}\left(32C_{of}^2C_r^2\right)\right] \Big/ \left[C_{of}^2C_r^2\left\{S_t\left(2+S_t\right)^{\frac{1}{2}}\right\}\left(2+S_t\right)^3\right]$$

$$b_3 = \left[\frac{1}{9}\begin{pmatrix} -10C_{of}C_r^2 - \frac{26}{3}C_{of}^2C_r + 2C_r^2 - \\ \frac{16}{9}C_{of}^2 + 26C_{of}^2C_r^2 + \frac{14}{3}C_{of}C_r \end{pmatrix}S_t^4 + \frac{1}{9}\begin{pmatrix} 156C_{of}^2C_r^2 + \frac{52}{3}C_{of}C_r + 8C_r^2 - \\ \frac{32}{3}C_{of}^2 - 52C_{of}^2C_r - 50C_{of}C_r^2 \end{pmatrix}S_t^3 + \frac{1}{9}\begin{pmatrix} 8C_r^2 + 320C_{of}^2C_r^2 + 16C_{of}C_r - \\ 16C_{of}^2 - \frac{340}{3}C_{of}^2C_r - 80C_{of}C_r^2 \end{pmatrix}S_t^2 + \right.$$

$$\left. + \frac{1}{9}\left(240C_{of}^2C_r^2 - 40C_{of}C_r^2 - 88C_{of}^2C_r\right)S_t + \frac{1}{9}\left(32C_{of}^2C_r^2\right)\right] \Big/ \left[C_r^2S_t\left\{S_t\left(2+S_t\right)^{\frac{1}{2}}\right\}\left(2+S_t\right)^2\right]$$

3.2 Numerical solution for all times

As stated, the starting values of ξ and θ_e in neighborhood of $\tau \to 0$ i.e $\tau = 10^{-4}$ are calculated from above solutions of small times. They are then employed in Runge-Kutta method to calculate numerical values of ξ and θ_e for all times.

Note that since the growth of the frozen layer, ξ with its subsequent melting may not be the same as the rate of increase of temperature of the additive, the faster rise of the later than the earlier permits the additive to attain the melting temperature of the bath material before the frozen layer completely melts. In such a situation the temperature of the additive and the melting front of the remaining frozen layer become at the melting temperature of the bath material. This results in the entire remaining frozen layer and the additive including its interface between the additive and the frozen layer to be at the melting temperature. Beyond the time of this happening, the convective heat from the bath is utilized only to melt the remaining frozen layer. The equation that regulates such a melting is provided by

$$-\frac{1}{S_t}\frac{d\xi}{d\tau} = B_{im}\left(\theta_b - 1\right) = \frac{1}{BC_{of}} = \frac{1}{C_{ofm}} \tag{20a}$$

This equation can be also obtained directly from Eq.(20) once $\theta_e = 1$ is substituted. Its closed-form solution is

$$\xi = \xi_r - \frac{S_t}{C_{ofm}}\left(\tau - \tau_r\right) \tag{20b}$$

It satisfies the condition $\xi = \xi_r$, $\tau = \tau_r$

Here, ξ_r denotes the thickness of the remaining frozen layer at the time, τ_r of the onset of the above occurrence. It readily gives the total time of freezing and melting once ξ becomes C_r.

Special cases: Bath temperature close to freezing temperature of the bath material, $T_b \to T_{mf.}$

In this situation the convective heat supplied by the bath becomes zero, $h(T_b - T_{mf}) = 0$ giving $BC_{of} = C_{ofm} = \infty$. Its application reduces Eq.(12) to

$$\frac{d}{d\tau}\left[\begin{array}{l} \frac{1}{2}\left(\xi^2 - C_r^2\right) + \left(\theta_e - 1\right)\cdot \\ \cdot\left\{\begin{array}{l} \frac{C_r}{2}\left(\xi - C_r\right) + \\ + \frac{1}{6}\left(\xi - C_r\right)^2 \end{array}\right\} - \frac{\xi^2}{2}\left(1 + \frac{1}{S_t}\right) \end{array}\right] = \frac{C_r\left(\theta_e - 1\right)}{\xi - C_r} \tag{21}$$

whereas Eq.(16) takes the form

$$\begin{aligned} &\frac{d\xi}{d\tau}\left(\xi - C_r\right)\left[\left(\theta_e - 1\right)\left\{\frac{1}{2}C_r + \frac{1}{3}\left(\xi - C_r\right)\right\} - \frac{\xi}{S_t}\right] = \\ &= \left(\theta_e - 1\right)\left\{C_r + C_r\left(\xi - C_r\right) + \frac{1}{3}\left(\xi - C_r\right)^2\right\} \end{aligned} \tag{22}$$

Using Eq.(14), Eq.(21) is transformed to

$$\frac{d}{d\tau}\left[\begin{array}{l} \frac{1}{2}\left(\xi^2 - C_r^2\right) + \left(\theta_e - 1\right)\left\{\begin{array}{l} \frac{C_r}{2}\left(\xi - C_r\right) + \\ + \frac{1}{6}\left(\xi - C_r\right)^2 \end{array}\right\} - \\ -\frac{\xi^2}{2}\left(1 + \frac{1}{S_t}\right) + \frac{C_r}{2}\left(\theta_e - 1\right) \end{array}\right] = 0 \tag{23}$$

giving closed-form solution between θ_e and ξ

$$\frac{1}{2}\left(\xi^2-C_r^2\right)+\left(\theta_e-1\right)\left\{\frac{C_r}{2}\left(\xi-C_r\right)+\frac{1}{6}\left(\xi-C_r\right)^2\right\}-$$
$$-\frac{\xi^2}{2}\left(1+\frac{1}{S_t}\right)+\frac{C_r}{2}\left(\theta_e-1\right)=C \tag{24}$$

For $\xi=\xi_r$, $\theta_e=0$

$$-\frac{\xi^2-C_r^2}{2}\left(1+\frac{1}{S_t}\right)+\frac{C_r}{2}+\frac{C_r}{2}\left(\theta_e-1\right)=0$$

Employing it, Eq.(24) becomes

$$\frac{1}{2}\left(\xi^2-C_r^2\right)+\left(\theta_e-1\right)\left\{\frac{C_r}{2}\left(\xi-C_r\right)+\frac{1}{6}\left(\xi-C_r\right)^2\right\}-$$
$$-\frac{\xi^2-C_r^2}{2}\left(1+\frac{1}{S_t}\right)+\frac{C_r}{2}+\frac{C_r}{2}\left(\theta_e-1\right)=0 \tag{25}$$

It satisfies the initial condition, $\tau=0$, $\xi=C_r$, $\theta_e=0$ and provides

$$\theta_e=1+\frac{-\left\{C_r-\frac{\xi^2-C_r^2}{S_t}\right\}}{\left\{C_r+C_r\left(\xi-C_r\right)+\frac{1}{3}\left(\xi-C_r\right)^2\right\}} \tag{26}$$

Case-I: If the latent heat of fusion released due to freezing of the bath material conducted to the additive raises the interface temperature θ_e to the freezing temperature of the bath material, $\theta_e=1$ no more freezing of the bath material occurs resulting in providing maximum frozen layer thickness, ξ_{max}. These convert Eq.(26) to

$$C_r=\frac{\xi_{\max}^2-C_r^2}{S_t} \tag{27}$$

It is cast in the following format

$$\xi_{\max}^*=\frac{\xi_{\max}-C_r}{S_t}=\frac{C_r}{S_t}\left[\sqrt{1+\frac{S_t}{C_r}}-1\right] \tag{28}$$

Note that under the condition of the bath temperature, $T_b>T_{mf}$, the growth of the maximum thickness of the frozen layer is smaller than that obtained from Eq.(28). It happens because the part of the latent heat of fusion supplied to the additive is replaced by the convective heat of the bath.

Eq.(28) can be also obtained once an energy balance between the latent heat of fusion evolved due to freezing of the bath material over the cylindrical additive and absorption of this heat to raise the temperature of the additive to the freezing temperature of the bath material is invoked. It gives

$$\pi r_0^2 l C_a\left(T_{mf}-T_{ai}\right)=\pi\left(r_{mf\,\max}^2-r_0^2\right)l\rho L \tag{29}$$

In nondimensional form it becomes

$$C_r=\frac{\xi_{\max}^2-C_r^2}{S_t} \tag{30}$$

It is rearranged as

$$\xi_{\max}^*=\frac{\xi_{\max}-C_r}{S_t}=\frac{C_r}{S_t}\left[\sqrt{1+\frac{S_t}{C_r}}-1\right] \tag{31}$$

and validates Eq.(28) derived from the prime analysis for $T_b\rightarrow T_{mf}$. It may be noted that exactly the same expression was derived in the previous study [3] for a spherical additive immersed in the bath.

Case - II : For the interface temperature, remaining below the freezing temperature of the bath material ($\theta_e<1$) , the time variant frozen layer thickness, (ξ-C_r) can be found once Eq.(26) is substituted in Eq.(22) providing

$$\left(\xi-C_r\right)\left[\frac{\left\{-C_r-\frac{\xi^2-C_r^2}{S_t}\right\}\left\{\frac{C_r}{2}+\frac{1}{3}\left(\xi-C_r\right)\right\}}{C_r+C_r\left(\xi-C_r\right)+\frac{1}{3}\left(\xi-C_r\right)^2}-\frac{\xi}{S_t}\right]\frac{d\xi}{d\tau}=$$
$$=-C_r+\frac{1}{S_t}\left(\xi^2-C_r^2\right)$$

when it is rearranged it becomes

$$\left(\xi-C_r\right)\left[\frac{\frac{C_r}{2}+\frac{1}{3}\left(\xi-C_r\right)}{C_r+C_r\left(\xi-C_r\right)+\frac{1}{3}\left(\xi-C_r\right)^2}-\right.$$
$$\left.-\frac{\xi}{S_t\left(-C_r+\frac{\xi^2-C_r^2}{S_t}\right)}\right]\frac{d\xi}{d\tau}=1 \tag{32}$$

To find its closed-form solution, it is written in standard integrable forms

$$\left[\frac{3C_r z+z^2}{2\left(3C_r-3C_r z+z^2\right)}+\frac{C_r z+z^2}{C_r S_t-2C_r z-z^2}\right]\frac{dz}{d\tau}=1 \tag{33}$$

where $z=\xi-C_r$

Satisfying the initial condition $\tau=0$, $\xi=C_r$ and $z=0$, its closed-form solution becomes

$$\tau=-\frac{3}{4}\ln\left(1+z+\frac{z^2}{3C_r}\right)+\frac{1}{4}A_1\ln\left\{\frac{4z+6C_r-2A_1}{4z+6C_r+2A_1}\right\}$$
$$\cdot\left\{\frac{6C_r+2A_1}{6C_r-2A_1}\right\}+\frac{C_r}{2}\ln\left(1+\frac{z}{S_t}+\frac{z^2}{C_r S_t}\right)+$$
$$+\frac{1}{2}A_2\left\{\frac{z+C_r-A_2}{z+C_r+A_2}\right\}\left\{\frac{C_r+A_2}{C_r-A_2}\right\} \tag{34}$$

Here,

$$A_1=\sqrt{9C_r^2-12C_r}\,,\quad A_2=\sqrt{C_r^2+C_r S_t}$$

For certain values of Cr and St, Eq.(34) readily provides the time for the growth of the frozen layer thickness whereas Eq.(26) gives the corresponding rise in the interface temperature, θ_e.

Validity:

To validate the present problem, the convective heat available from the bath is assumed to be more

than the heat conducted to the additive resulting in no growth of frozen layer. This reduces the present problem to the transient heating of the cylindrical additive of negligible thermal resistance by convective heat supplied from the surrounding bath. It is exactly the same that appeared in the literature [22, 23, 29]. In the present format it is given by

$$\left(1-\frac{\theta_e}{\theta_b}\right)=e^{-B_i\tau} \tag{35}$$

4. Results and discussions

Mathematical model evolved in a lump-integral form for freezing and melting of the bath material onto the surface of a cylindrical additive with its thermal resistance negligible with respect to that of the bath and the frozen layer exhibits the dependence of this phenomenon on the non-dimensional parameters- the Stefan number, S_t the modified conduction factor, C_{ofm} and the heat capacity-ratio, C_r. The Stefan number denotes the phase-change parameter and is the ratio of sensible heat and latent heat of fusion of the bath material. When its value is low, it signifies the bath material of high latent heat of fusion resulting in growth of small thickness of the frozen layer despite liberation of large amount of heat due to freezing for the same heat to be conducted to the additive. The modified conduction factor is the product of property-ratio, B and the conduction factor, C_{ofm} (C_{ofm} =B C_{of}). The later represents the ratio between the heat conducted, $K_a(T_{mf}-T_{ai})/r_o$ to the additive due to the difference of freezing temperature of the bath material and the initial temperature of the additive, and the convective heat, $h(T_b-T_{mf})$ supplied from the bath. Its values range from 0 to ∞. Zero implies the preheated additive at the freezing temperature of the bath material allowing no conductive heat transfer to the additive with no growth of the frozen layer. Infinity, ∞ indicates the bath to be at the freezing temperature of the bath material resulting in no supply of convective heat from the bath. Here, only freezing around the surface of the additive takes place with no subsequent melting. Depending on the values of B, smaller or greater than one, the modified conduction factor becomes less or more than the conduction factor. The small heat capacity-ratio, (C_r<1) signifies the absorption of large heat within the heated region of the additive than that in the frozen layer. Table1 presents the values of these independent parameters for various bath-cylindrical additive systems often used in practice.

Graphs for the time variant freezing and melting, ξ-C_r and the interface temperature, θ_e are displayed in Figs.2, 4 and 6. Here, the total time of freezing and melting is the time between the start of the freezing and the completion of the melting of the frozen layer. The time of the growth of the maximum thickness of the frozen layer is denoted by the time taken to grow this thickness whereas the time of the complete melting of the frozen layer is represented by the difference between the total time for freezing and melting and the time taken to grow the maximum thickness of the frozen layer. All the figures exhibit similar behavior. An early part of any graph of freezing is attained swiftly after the immersion of the additive in the bath whereas the melting of the frozen layer is slow with the later portion of the melting follows a linear behavior with time. This later behavior is owing to the interface temperature, θ_e rapidly rising to the freezing temperature of the bath material before the complete melting of the frozen layer. In such a situation, the remaining frozen layer including the interface temperature and the freezing front to be at the freezing temperature of the bath material. Due to this it does not absorb the convective heat supplied by the bath as sensible heat rather it is completely utilised in melting this layer. It is predicted by Eq.(20b) and varies linearly with time. This type of behavior was also reported in the previous study [12] for freezing and melting of the bath material onto the spherical shaped additive.

4.1 Influence of Modified Conduction Factor, C_{ofm}

Fig.2 shows the effect of the modified conduction factor, C_{ofm} upon the time dependent frozen layer thickness, ξ-C_r and the instant interface temperature, θ_e for certain values of the Stefan number, S_t and the

Table 1. *Thermo-physical properties of typical Bath- Solid system and their dimensionless parameters.*

Bath Material								Solid Additive				Non-Dimensional parameters				
	K_m W / mk	ρ_m Kg/m^3	C_{pm} J/kgk	L_m x10^{-3} J/ kg	T_{mf} ^{0}C	T_b ^{0}C	h W/ m^{2}k		K_a W / mk	ρ_a Kg/ m^3	C_{pa} J / kgk	θ_b	B	*B_i	C_{ofm}	S_t
Hot metal [12]	35	6850	670	275.7	1150	1500	1000	Ferro-mang. [12]	75	7200	700	1.31	0.42	0.067	20.3	2.71
Cast- Iron ~4%C [23]	51.9	7304	417	275.7	1160	1550	1500	Nickel [22]	90	8906	449	1.08	0.44	0.083	63	2.11
Slag [3]	1.063	2890	920	544	1500	1600	40	DRI [3]	2.13	2600	820	1.07	0.62	0.094	97	2.48

** Based on radius of additive r_o =.01m and T_{ai}=35^{0}C*

heat capacity-ratio, C_r . For each C_{ofm} , the behaviour of ξ-C_r and θ_e is similar to those stated earlier. But due to increase in C_{ofm}, the maximum frozen layer thickness, its time of formation and the total time of freezing and melting increase. The interface temperature, θ_e falls almost on the same graph but the time of attaining the freezing temperature (θ_e=1) of the bath material gets delayed. The frozen layer does not melt completely at this temperature θ_e=1. As described earlier the remaining entire frozen layer becomes at θ_e=1. The feature just stated is expected because the heat conducted to the additive is sum of the convective heat and the latent heat of fusion liberated by freezing of the bath material onto the additive, increased C_{ofm} reduces the convective heat resulting in its compensation by release of more latent heat of fusion from the growth of large thickness of the frozen layer.

For a prescribed bath material represented by S_t and C_r, the total time of freezing and melting τ_t, the time τ_{max} required for the growth of maximum frozen layer thickness developed with modified conduction factor, C_{ofm} appear in Fig.3. They indicate that these times and the maximum frozen layer thickness rapidly increase once C_{ofm} rises from zero to two ($0 \le C_{ofm} \le 2$). For C_{ofm}>2, they assume almost a linear behaviour. However, the maximum frozen layer thickness and its time of formation increase insignificantly. Rather these two acquire an asymptotic behaviour. The total time, τ_t for freezing and melting with respect to increasing C_{ofm} is also linear but the time of melting, the difference between τ_t and τ_{max} becomes progressively much greater than that of the freezing. This is possibly due to phenomenon of melting less responsive to increasing C_{ofm} and in turn, diminishing convective heat transfer. For reduction in the total time of freezing and melting, C_{ofm}<2 needs to be maintained in order to decrease the time of melt preparation and, in turn the manufacturing time.

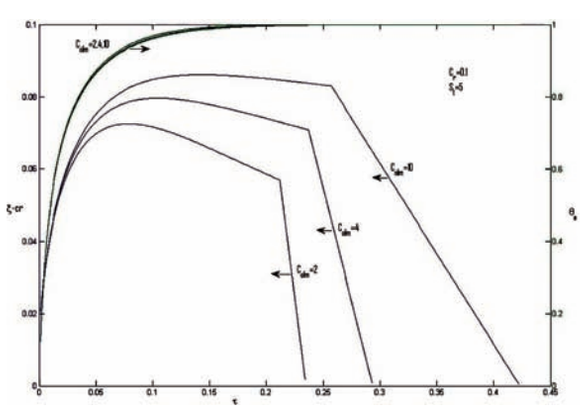

Figure 2. *Time, τ variant freezing & melting (ξ-C_r) and the interface temperature, θ_e for different values of modified conduction factor, C_{ofm} Stefan number, S_t and heat capacity-ratio, C_r are taken as parameters.*

4.2 Effect of Heat Capacity-Ratio, C_r

In the Fig.4, the influence of heat capacity-ratio, C_r upon the growth of the frozen layer, ξ-C_r with its melting and the rise of the interface temperature, θ_e with time for prescribed values of the Stefan number, St and the modified conduction factor, C_{ofm} is exhibited. For all C_r ($0.1 \le C_r \le 10$), their behavior is similar to those described in earlier section. However, when C_r decreases, the maximum thickness of the frozen layer, time taken for its growth and the total time of the freezing and melting reduce whereas the rise in the interface temperature, θe to reach the freezing temperature (θ_e=1) of the bath material is faster. At such a temperature, the frozen layer that grew does not melt completely rather the entire left-over frozen layer attains the freezing temperature of the bath material. Beyond this occurrence, the convective heat from the bath melts only the left-over frozen layer. The melting follows a linear behavior with time, Eq.(20b). This characteristic is realistic

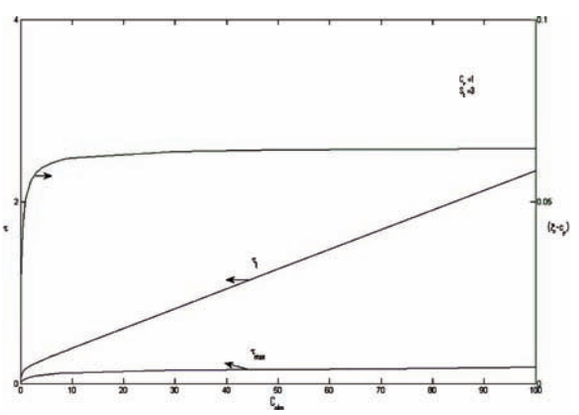

Figure 3*. Variation of maximum frozen layer thickness, (ξ-C_r), its growth time, τ_{max} and total time, τ_t of freezing and melting with modified conduction factor, C_{ofm} for certain values of C_r and S_t.*

because decreased C_r reduces the absorption of sensible heat by the frozen layer due to which more convective heat is available for conducting to the additive. Consequently, less latent heat of fusion is required to balance the conductive heat. It is met by freezing a small thickness of the bath material onto the additive.

Heat capacity-ratio, C_r dependent total time of freezing and melting τ_t, the time τ_{max} for the development of maximum frozen layer thickness and the formation of this thickness are exhibited in Fig.5 for certain bath material and its condition denoted by

S_t and C_{ofm}, respectively. All swiftly rise once C_r is allowed to vary between 0 to 1 ($0 \leq C_r \leq 1$). For $C_r > 1$, they remain also constant. It is inferred that to have lower total time of freezing and melting and consequently, the manufacturing time, C_r is required to be kept below one ($C_r < 1$).

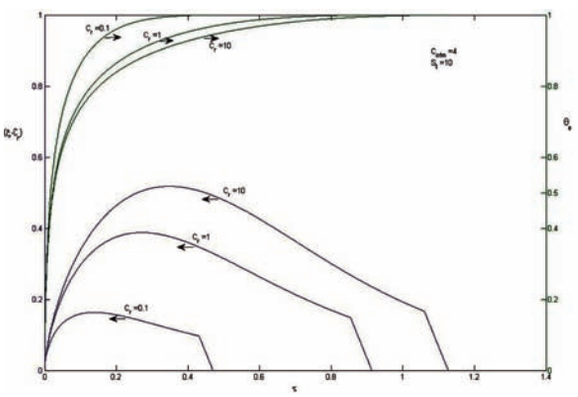

Figure 4. *Effect of heat capacity-ratio, C_r upon freezing & melting (ξ- C_r) and build up of interface temperature, θ_e with time, τ for certain values of Stefan number, S_t and modified conduction factor, C_{ofm}.*

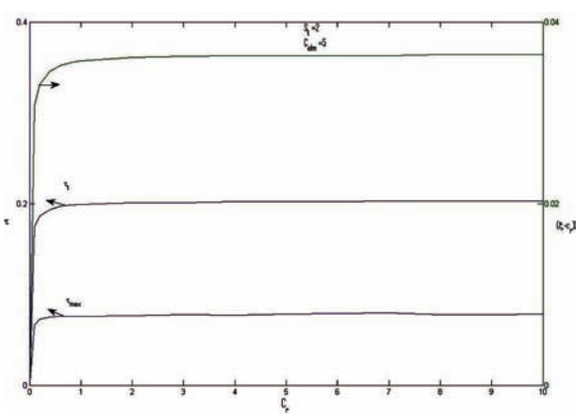

Figure 5. *Heat capacity-ratio, C_r dependent maximum frozen layer thickness, (ξ-C_r), its growth time, τ_{max} and total time of freezing with its subsequent melting, τ_t for certain values of S_t and C_{ofm}.*

4.3 Impact of Stefan number, S_t

For certain values of C_{ofm} and Cr, time-dependent growth of the frozen layer, ξ-C_r with its subsequent melting and associated rise in the interface temperature, θ_e are exhibited in Fig.6. The Stefan number, S_t is assumed to be a parameter. Their behavior for each St is similar to those already described. However, decreasing S_t diminishes the maximum frozen layer thickness, its time of formation and total time of freezing and melting. The

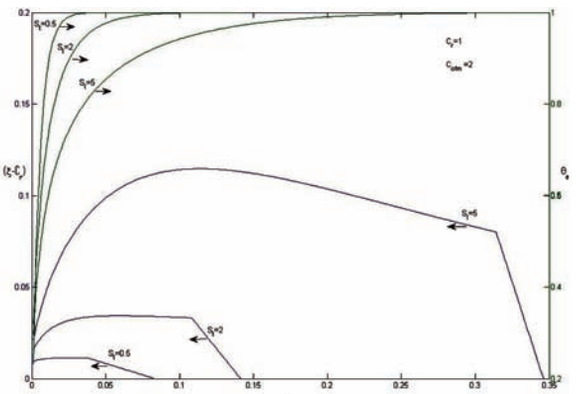

Figure 6. *Time, τ dependent freezing & melting (ξ- C_r) and the increase in interface temperature, θ_e for different values of Stefan number, S_t for prescribed values of modified conduction factor, C_{ofm} and heat capacity-ratio, C_r.*

rise in interface temperature is faster allowing it to attain the melting temperature of the bath material earlier than the complete melting of the frozen layer. As a result, the remaining frozen layer becomes at the melting temperature and does not absorb the convective heat as the sensible heat but this heat melts the remaining frozen layer. The melting assumes linearity with time, Eq.(20b). These behaviors are anticipated since lower St is representative of large latent heat of fusion of the freezing bath material allowing the growth of a smaller frozen layer thickness. It releases enough latent heat of fusion to meet the conductive heat which is equal to the latent heat of fusion and the convective heat available from the bath.

Fig.7 depicts the behavior of the Stefan number, S_t variant total time of freezing and melting, τ_t, the maximum frozen layer thickness with its time of growth. They state that τ_t and the maximum frozen

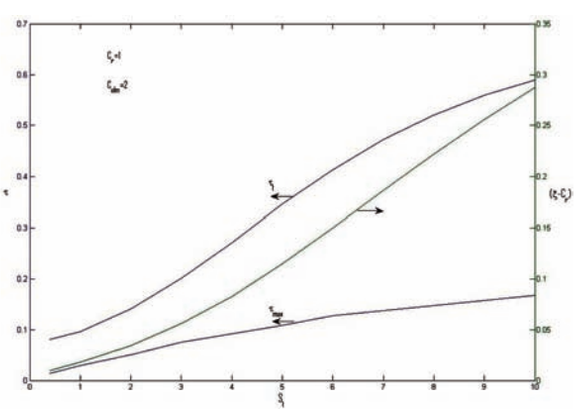

Figure 7. *Variation of maximum frozen layer thickness, (ξ-C_r), its time for growth, τ_{max} and total time, τ_t of freezing & melting with Stefan number, S_t for certain values of heat capacity-ratio, C_r and modified conduction factor, C_{ofm}.*

layer thickness increase with a faster rate for lower S_t and τ_t assumes linearity for $S_t<2$ whereas that of the maximum frozen layer thickness for $S_t<4$, but the time required for the growth of the maximum frozen layer thickness is linear in the entire range of S_t ($0\leq S_t\leq 10$). In view of these predictions, need for the lower total time of freezing and melting and associated manufacturing time for a given additive-melt bath system, S_t of the bath material is decreased only by increasing the initial temperature of the additive, T_{ai} in $S_t=C_{pm}(T_{mf}-T_{ai})/L_m$.

4.4 The application of the model to the manufacturing practices:

This model provides the governance of the freezing and melting of the bath material onto a cylindrical additive of negligible thermal resistance with that of the bath by the independent parameters, St, C_r and C_{ofm}. Here, the cylindrical ferromanganese additive-hot metal bath system, the thermo-physical properties of which appear in Table1 is considered. This Table1 for such a system provides St=2.71, Bi=0.067, C_r=0.91, B=0.425 and C_{ofm}=20.3 when the radius of this additive is 0.01m and heat transfer coefficient is 1000W/m^{2}K. Bi=0.067<0.1 signifies that the thermal resistance of this cylindrical additive is negligible with that of the frozen bath material. Using these values, the numerical solutions of the present model give

maximum thickness of the frozen layer developed, $(\xi_{max}-C_r)= 0.0542$

time to develop this maximum frozen layer thickness, $\tau_{max}=0.1161$

total time of freezing and melting, also called shell period= $\tau_t=0.5671$

Using the thermo-physical properties data from Table1 and nomenclature for these, they become respectively,

$$\xi_{\max}-C_r=\frac{C_m r_{\max}}{C_a r_0}-\frac{C_m}{C_a}=C_r\left(\frac{r_{\max}}{r_0}-1\right)= \\ =0.91\left(100r_{max}-1\right) \tag{36}$$

$$\tau_{\max}=\left(\frac{KC_m}{C_a^2 r_0^2}\right)\quad t_{max}=0.0632t_{max} \tag{37}$$

$$\tau_t=\left(\frac{K_m C_m}{C_a^2 r_0^2}\right)\quad t_t=0.0632t_t \tag{38}$$

Using the above values of $(\xi_{max}-C_r)$ in Eq.(36), τ_{max} in Eq.(37) and t_t in Eq.(38) provide the maximum frozen layer thickness, 6×10^{-4}m, time of its formation $t_{max}\cong$2s and the total time of the freezing and melting, $t_t\cong$9s. For the spherical ferromanganese additive of same radius-hot metal system having their resistances comparable, the previous study [12] reported the time of the freezing and melting of the bath material onto the additive about 15s. It is higher because such resistances decelerate the phenomenon of the freezing and melting.

4.5 Comparison with experimental results of the literature

In the literature, experimental results of the present problem are not available. However, for the additive having its thermal resistance comparable with that of the bath material experimental data were provided by Sismanis and Argyropoulos [30] for dissolution of titanium, zirconium, niobium and tantalum cylinders in steel melt. Their dissolution was preceded by the freezing and melting of the steel melt onto them. From their experimental and predicted data for the interface and centerline temperature of the niobium cylinder of 2.54×10^{-2}m diameter and 18×10^{-2}m length they inferred that the radial temperature was almost uniform in the cylinder. This property permits to assume the niobium cylinder of negligible thermal resistance. Owing to this fact, the interface temperature obtained from the present problem can be compared with that of the niobium cylinder-steel melt bath system. The data of this system [30] give Cr=2.236, B=1.278, St=4.346, θ_b=1.053, Bi=9.22 and C_{ofm} =3.465. For these values the interface temperature distribution with time is calculated for the present problem and compared with that of the niobium [30] in Fig.8.

It is observed that during the initial time of the freezing of the steel melt around the niobium cylinder the agreement is close. With the elapse of time, the

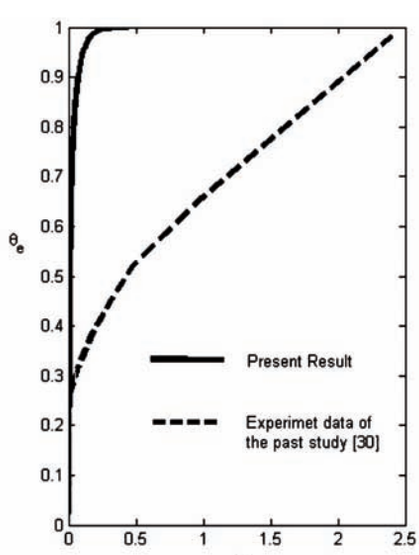

***Figure 8**. Comparison of the present numerical results for the interface temperature, θ_e related to niobium-steel melt system with the experimental data of the literature [30].*

frozen layer grows to its maximum thickness and subsequently melts but the interface temperature continues to rise to acquire the freezing temperature of the steel melt. In this time region, the time to attain the same interface temperature is lesser for the present problem than that of the literature [30]. This is due to the fact that the comparative resistances of the cylindrical niobium additive and steel melt bath impedes the rate of the rise of the interface temperature that takes place in the niobium additive of negligible thermal resistance with respect to that of the steel bath in the present work.

5. Conclusions

The mathematical model devised in a lump-integral format for the unsteady axisymmetric freezing and melting of the bath material around the cylindrical solid additive of negligible thermal resistance is controlled by independent nondimensional parameters, the Stefan number, S_t, the heat capacity-ratio, C_r and the modified conduction factor, C_{ofm}. The model predicts that decreasing C_{ofm} reduces the maximum frozen layer thickness, its time of growth and the time of freezing and melting. These are further decreased once the Stefan number is reduced. The interface temperature, θ_e reaches the freezing temperature of the bath material earlier than the melting of the frozen layer. In this situation, the convective heat only melts this remaining layer. For the bath to be at its material freezing temperature, the maximum frozen layer thickness, $\xi^*_{max} = C_r\left(\sqrt{1+S_t/C_r}-1\right)/S_t$ when θ_e attains the bath material freezing temperature by the latent heat of fusion evolved by the freezing of the bath material. The instant problem is validated by transforming it to convective heating of the additive of negligible thermal resistance.

Acknowledgement

The authors acknowledge Dr. R.P. Singh, Professor of Metallurgy and Material Science of National Institute of Technology, Jamshedpur (India) for providing the Matlab facility.

References

[1] R.P.Singh and A. Prasad , Mathl. Comput. Modelling, 37 (2003) 849-862.

[2] S.Sanyal, S.Chandra, S.Kumar, G.G.Roy, ISIJ Int., 44 (2004) 1157-1166.

[3] Q.Jiao and J.Themlis, Can. Metall. Q., 32 (1993) 75-83.

[4] J. Li, G. Brooks and N. Provatas, Metall. Mater. Trans. B, 36B (2005) 293-302.

[5] L. Pandelaers, F. Verhaeghe, D. Barrier, P. Gardin, P. Wollants and B. Blanpain, Ironmaking and Steelmaking, 37 (7) (2010) 516-521.

[6] L. Pandelaers, F. Verhaeghe, B. Blanpain, P. Wollants and P. Gardin, Metall. Mater. Trans. B, 40B (2009) 676-684.

[7] S.A. Arigyropoulos and R.I.L. Guthrie, Metall.Trans. B, 15 (1) B (1984) 47-58

[8] S.A. Arigyropoulos and P.G. Sismansis, Metall. Trans. B, 22 (4) B (1991) 417-428.

[9] S.A. Arigyropoulos and P.G. Sismansis, Steel Research, 68 (8) (1997) 345-354

[10] S. Sanyal, S. Chandra, B.K.Jha, H.J.Billimoria, A. Choudhary and G.G.Roy, Tata Search, (2004) 190-199

[11] B. Zhou, Y. Yang, M. A. Reuter, Extraction and processing division meeting of TMS, 16-20 June, Lulea, Sweden, 2002, p.527-537

[12] R. Kumar, S. Chandra and A. Chatterjee, Tata Search, (1997) 78-85.

[13] L. Zhang, Steel Research, 67 (1996) 466-74.

[14] L. Zhang and F. Oeters, Steel Research, 70 (1999) 128-134.

[15] N. Bannenberg, H. Lachmund, F. Oeters and L. Zhang, Stahl und Eisen 119 (2) (1999) 37-44.

[16] L. Zhang and F. Oeters, Melting and mixing of alloying agents in steel melts -Methods of mathematical modelling, Publisher Stahleisen, Germany, 1998.

[17] U. C. Singh, A. Prasad and Arbind Kumar, Metall. Mater. Trans. B, 42B (2011) 800-806.

[18] R.P.Singh and A. Prasad, Ironmaking and Steelmaking, 32 (2005) 411-417.

[19] U. C. Singh, A. Prasad, A. Kumar, J. Min. Metall. Sec. B- Metall., 48 (1) B (2012) 11-23.

[20] F. Oeters, L. Zhang, C. Hauler and J. Leitner, Steel Research, 71(10) (2000) 381-390.

[21] J. Leitner, C. Hauler, F. Oeters, L. Zhang and S. Eriksson, Stahl und Eisen, 120(11) (2000) 69-74.

[22] M.N.Ozisik, Heat Transfer, A Basic Approach, McGrawHill, NewYork, 1985, P.101.

[23] E.R.G. Eckert and R.M. Drake, Analysis of Heat and Mass Transfer, International Student edition McGrawHill Kogakusha, Tokyo, 1972.

[24] A. P. Roday and M. J. Kazmierczak, Int. Rev. Chem. Eng., 1(1) (2009) 100-108.

[25] A. P. Roday and M. J. Kazmierczak, Int. Rev. Chem. Eng., 1(1) (2009) 87-99.

[26] A. Prasad and S.P. Singh, Transaction of the ASME, 116 (1994) 218-223.

[27] A. Prasad, J. Spacecraft Rockets, 17 (1980) 474-477.

[28] B.T.F. Chung and L.T.Yeh, J. Spacecraft Rockets, 12 (1975) 329-330

[29] F. Kreith, Principles of Heat Transfer, 3rd edition, Intext Education Publishers, New York, USA, 1973.

[30] P.G. Sismanis and S.A. Argyropoulos, Met. Soc. Pennsylvania, 1987 483-508.

Appendix - NOMENCLATURE

R_0 radius of the cylindrical shaped solid additive, m

B property ratio, (K_mC_m/K_aC_a)

B_i Biot number, (hR_0/K_a)

B_{im} Modified Biot number, $(hR_0/K_a)*(K_aC_a/K_mC_m)$

C_a heat capacity of the cylindrical additive, $Jm^{-3}K^{-1}$

C_m heat capacity of the frozen layer, $Jm^{-3}K^{-1}$

C_{of} conduction factor, $(1- \theta_{ai})/ B_i (\theta_b -1)$

C_r Heat capacity ratio, C_m/C_a

R_a radius of the heat penetration front in the additive at any time, m

R_m radius of the frozen layer front onto the additive at any time, m

h heat transfer coefficient, $Wm^{-2}K^{-1}$

K_a thermal conductivity of the additive, $Wm^{-1}K^{-1}$

K_m thermal conductivity of the frozen layer, $Wm^{-1}K^{-1}$

L_m latent heat of fusion of the frozen layer, JKg^{-1}

Q_m heat transfer from the frozen layer to the additive, Wm^{-2}

Q_{mn} non-dimensional heat transfer from the frozen layer to the additive, $Q_mR_0/ K_a (T_{mf} -T_{ai})B$

S_t Stefan number, $C_m(T_{mf} -T_{ai})/ L_m \rho_m$

t time, s

t_{mc} time for freezing and its subsequent melting, s

T temperature, K

T_a temperature of the additive, K

T_{ai} initial temperature of the additive, K

T_{af} freezing or melting temperature of the additive, K

T_b bulk temperature of the bath material, K

T_e instant equilibrium temperature at the interface between the additive and the frozen layer, K

T_{em} instant equilibrium temperature at the interface between the additive and the frozen layer when the frozen layer completely melted, K

T_{mf} freezing or melting temperature of the frozen layer, K

r_a radius within the heat penetration region in the additive, m

r_m radius within the frozen region, m

α_a thermal diffusivity of the additive, m^2s^{-1}

α_m thermal diffusivity of the frozen layer, m^2s^{-1}

ξ non-dimensional radius of the frozen layer front at any time, (C_mR_m/ C_aR_0)

ξ_a non-dimensional radius in the heat penetration region in the additive, (r_a /R_0)

ξ_m non-dimensional radius within the frozen layer region, $(C_m r_m/ C_aR_0)$

η non-dimensional radius of the heat penetration front in the additive at any time, (R_a/R_0)

ρ_m density of the frozen layer, Kgm^{-3}

θ non-dimensional temperature, $(T-T_{ai}/ T_{mf} - T_{ai})$

θ_a non-dimensional temperature of the additive at any time, $(T_a- T_{ai} / T_{mf-} T_{ai})$

θ_{af} non-dimensional freezing or melting temperature of the additive, $(T_{af}-T_{ai} /T_{mf} -T_{ai})$

θ_b non-dimensional bulk temperature of the bath material, $(T_b -T_{ai} /T_{mf} - T_{ai})$

θ_e non-dimensional instant equilibrium temperature at the interface between the additive and the frozen layer, $(T_e-T_{ai} /T_{mf} - T_{ai})$

τ non-dimensional time, $(K_mC_m/C_a^2 R_0^2)t$

q_{na} non-dimensional heat transfer from interface to the additive, $q_ar_0/ K_a (T_{mf} -T_{ai})$